arXiv:cond-mat/0602597v2 [cond-mat.mes-hall] 4 Aug 2006

Magnetic field-assisted manipulation and entanglement of Si spin qubits

M.J. Calderón,[1] Belita Koiller,[1,2] and S. Das Sarma[1]
[1]*Condensed Matter Theory Center, Department of Physics, University of Maryland, College Park, MD 20742-4111*
[2]*Instituto de Física, Universidade Federal do Rio de Janeiro, Caixa Postal 68528, 21941-972 Rio de Janeiro, Brazil*

(Dated: February 6, 2008)

Architectures of donor-electron based qubits in silicon near an oxide interface are considered theoretically. We find that the precondition for reliable logic and read-out operations, namely the individual identification of each donor-bound electron near the interface, may be accomplished by fine-tuning electric and magnetic fields, both applied perpendicularly to the interface. We argue that such magnetic fields may also be valuable in controlling two-qubit entanglement via donor electron pairs near the interface.

PACS numbers: 03.67.Lx, 85.30.-z, 73.20.Hb, 85.35.Gv, 71.55.Cn

Spin qubits in semiconductors (e.g. GaAs, Si) are among the most promising physical systems for the eventual fabrication of a working quantum computer (QC). There are two compelling reasons for this perceived importance of semiconductor spin qubits: (i) electron spin has very long coherence times, making quantum error correction schemes feasible as a matter of principle; (ii) semiconductor structures provide inherently scalable solid state architectures, as exemplified by the astonishing success of the microelectronics technology in increasing the speed and efficiency of logic and memory operations over the last fifty years (i.e. 'Moore's Law'). These advantages of semiconductor quantum computation apply much more to Si than to GaAs, because the electron spin coherence time can be increased indefinitely (up to 100 ms or even longer in the bulk) in Si through isotopic purification [1, 2, 3] whereas in GaAs the electron spin coherence time is restricted only to about 10 μs [1, 2, 4]. It is thus quite ironic that there has been much more substantial experimental progress [4] in electron spin and charge qubit manipulation in the III-V semiconductor quantum dot systems [5] than in the Si:P Kane computer architecture [6]. In addition to the long coherence time, the Si:P architecture has the highly desirable property of microscopically identical qubits which are scalable using the Si microelectronic technology. The main reason for the slow experimental progress in the Kane architecture is the singular lack of qubit-specific quantum control over an electron which is localized around a substitutional P atom in the bulk in a relatively unknown location. This control has turned out to be an impossibly difficult experimental task in spite of impressive developments in materials fabrication and growth in the Si:P architecture using both the 'top-down' and the 'bottom-up' techniques [7]. It is becoming manifestly clear that new ideas are needed in developing quantum control over single qubits in the Si:P QC architecture.

In this Letter we suggest such a new idea, establishing convincingly that the use of a magnetic field, along with an electric field, would enable precise identification, manipulation and entanglement of donor qubits in the Si:P quantum computer architecture by allowing control over the spatial location of the electron as it is pulled from its shallow hydrogenic donor state to the Si/SiO$_2$ interface by an electric field. Additionally, the magnetic field could be used to control the spatial overlap of the electronic wavefunctions in the 2D plane parallel to the interface (i.e. similar to a MOSFET geometry), thus enabling external manipulation of the inter-qubit entanglement through the magnetic field tuning of the exchange coupling between neighboring spin qubits [5].

Fig. 1 highlights the basic physical effects explored in our theoretical study: Substitutional P donors in Si, separated by R, are a distance d from an ideally flat Si/SiO$_2$ (001) interface. Uniform electric $\mathbf{F}$ and magnetic $\mathbf{B}$ fields are both applied along z. When a single P atom is considered ($R \to \infty$ limit), and in the absence of external fields, the active electron is bound to the donor potential well (W_D) forming a hydrogenic atom. If a uniform electric field is also present, an additional well is formed which tends to draw the donor electron toward the interface. The interface well (W_I) is triangular-shaped along z while in the xy 2D plane the confinement is still provided by the 'distant' donor Coulomb attraction. The ground-state wavefunctions for each well are given in Fig. 1(b). This corresponds to a particular value of the applied field, the critical field which we denote by $F = F_c(d)$, such that the expectation values of the energy for the W_I and W_D ground-eigenstates are degenerate. Fig. 1(c) shows how the system in (b) changes due to a magnetic field applied along z. The interface ground state wavefunction undergoes the usual 'shrinking' perpendicular to $\mathbf{B}$, and the energy at W_I is raised, while no significant changes occur at W_D. As a consequence, we find that by properly tuning $\mathbf{B}$ it is possible to control the electron location *along the applied magnetic field direction*, partially or completely reversing the effect of the electric field.

We base our quantitative description of this problem

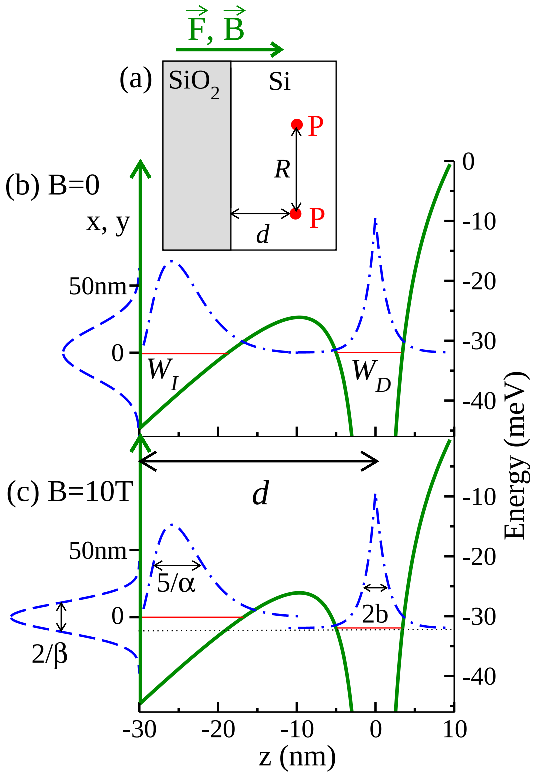

FIG. 1: (Color online) (a) Schematic configuration of donors in Si near the interface with an oxide barrier under applied electric **F** and magnetic **B** uniform fields. In (b) and (c), the thick lines show the electronic confining double-well potential: The interface well is labeled W_I and the donor well, W_D. The dashed lines give the decoupled ground-eigenfunctions in the wells, and the thin horizontal lines indicate the expectation value of the energy in each well. Results for $d = 30\,\mathrm{nm}$ and $F = 13.5\,\mathrm{kV/cm} \approx F_c(d)$, are given in (b) for $B = 0$ and in (c) for $B = 10\,\mathrm{T}$. Parameters defining typical wavefunction widths (see text) are indicated in (c). Magnetic field effects tend to be stronger for larger d, as the interface state is less affected by the strongly confining Coulomb potential at W_D.

on the single-valley effective-mass approximation, leading to the model-Hamiltonian [8, 9]

$$H = T + eFz - \frac{e^2}{\epsilon_1 r} + \frac{e^2 Q}{\sqrt{\rho^2 + (z+2d)^2}} - \frac{e^2 Q}{4(z+d)} \ . \quad (1)$$

The magnetic field vector potential, $\mathbf{A} = B\,(y, -x, 0)\,/2$, is included in the kinetic energy term, $T = \sum_{\eta=x,y,z} \hbar^2/(2m_\eta)\,\left(i\partial/\partial\eta + eA_\eta/(\hbar c)\right)^2$, where the effective masses $m_x = m_y = m_\perp = 0.191\,m$ and $m_z = m_\parallel = 0.916\,m$, account for the Si conduction band valley's anisotropy. The electric field defines the second term in H, the third and fourth terms describe the donor and its image charge potentials, while the last term is the electron image potential. The fourth term involves the lateral coordinate $\vec{\rho} = (x, y)$. The image-related terms are proportional to $Q = (\epsilon_2 - \epsilon_1)/[\epsilon_1(\epsilon_2 + \epsilon_1)]$, where $\epsilon_1 = 11.4$ and $\epsilon_2 = 3.8$ are the Si and SiO$_2$ static dielectric constants. It is convenient to rewrite the kinetic energy term as

$$T = T_0 + \frac{1}{8}\omega_c^2 \rho^2 + i\omega_c \left(y\frac{\partial}{\partial x} - x\frac{\partial}{\partial y} \right) \ , \qquad (2)$$

where T_0 is the kinetic energy for $B = 0$ and $\omega_c = eB/(m_\perp c)$. The second term allows interpreting the effect of the magnetic field as providing an additional parabolic potential in the xy plane, which increases the kinetic energy and enhances the lateral confinement of the electron wave-function. The last term in T gives zero or negligible contribution for the donor electron low-energy states being investigated, and will be neglected here.

We solve the double-well problem described by the model Hamiltonian in Eq. (1) in the basis of the uncoupled solutions to the individual wells W_I and W_D, obtained variationally from the *ansatz* [9]:

$$\begin{aligned} \Psi_I(\rho, z) &= f_\alpha(z) \times g_\beta(\rho) & (3) \\ &= \frac{\alpha^{5/2}}{\sqrt{24}}(z+d)^2\, e^{-\alpha(z+d)/2} \times \frac{\beta}{\sqrt{\pi}}\, e^{-\beta^2\rho^2/2} & \\ \Psi_D(\rho, z) &\propto (z+d)e^{-\sqrt{\rho^2/a^2 + z^2/b^2}} \ , & (4) \end{aligned}$$

where α, β, a and b are the variational parameters. The $(z+d)$ factors guarantee that the wavefunctions are zero at the interface ($z = -d$), as we assume that the insulator provides an infinite barrier potential. For $d > 6$ nm and $B = 0$, we find that a and b coincide with the Kohn-Luttinger variational Bohr radii for the isolated impurity ($d \to \infty$), where $a = 2.365$ nm and $b = 1.36$ nm.

As an illustration of the uncoupled wells variational solutions, we present in Fig. 1 the calculated wavefunctions for $d = 30$nm. The dash-dot lines correspond to $f_\alpha(z)$ and $\Psi_D(0, z)$, while the dashed lines on the left represent $g_\beta(\rho)$ for $\vec{\rho} = (x, 0)$ [or equivalently $(0, y)$]. It is clear from this figure that the four variational parameters define relevant length scales involved in the problem. In the presence of a magnetic field, there is an additional length scale (the magnetic length) given by $\lambda_B = \sqrt{\hbar c/(eB)}$ which defines the typical lateral confinement produced by the magnetic field alone, regardless of other potentials in the problem. The magnetic field effect is significant only for values of $B \gtrsim B_c$ such that $\lambda_B \lesssim c_\rho$ where c_ρ is the lateral confinement length in the absence of the field. For the donor potential well, $c_\rho \approx a = 2.365$ nm, so that the field required to appreciable affect the W_D-ground state eigenenergy or wavefunction is $B_c^D \sim 120$ T! On the other hand, for the W_I well, the confinement length at the interface for $B = 0$ is $1/\beta \sim 18.5$ nm so that a much smaller $B_c^I \sim 2$ T is sufficient to affect the interface ground state. The magnetic field strengths we consider here (up to 10 T) are not large enough to affect a or b, but important effects are obtained in lateral confinement at the interface as shown in Fig. 1 by comparison of $B = 0$ in (b) with $B = 10$ T in (c).

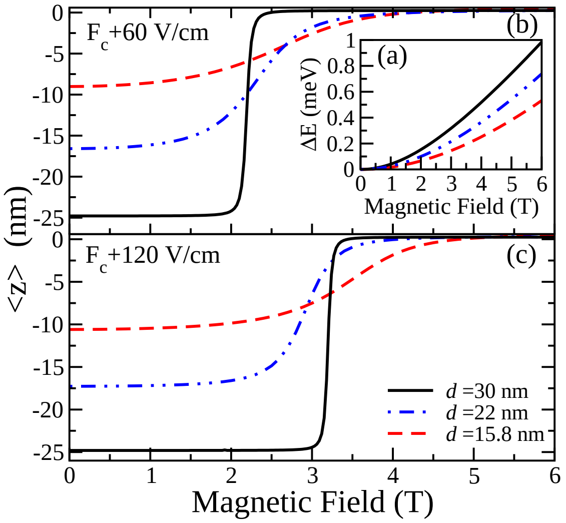

FIG. 2: (Color online) (a) Shift in the energy $\mathcal{E}_I$, associated with the interface state, versus magnetic field for three values of the donor distance to the barrier (d). The shift in energy of the donor state ($\mathcal{E}_D$) is negligible compared to these values and is not shown. (b) Expectation value of the z-position for the electronic ground state versus magnetic field. For each d the electric field is tuned to a value just above the critical field: $F = F_c + 60$ V/cm. The electron starts at a position close to the interface and moves parallel to the magnetic field and against the electric field ending up at the donor well. The values of the critical electric field at each distance are F_c(15.8 nm) $= 27.44$ kV/cm, F_c(22 nm) $= 18.85$ kV/cm, F_c(30 nm) $= 13.44$ kV/cm. (c) Same as (b) for $F = F_c + 120$ V/cm.

The expectation value of the energy for each well ground state, $\mathcal{E}_j = \langle\Psi_j|H|\Psi_j\rangle_{(j=I,D)}$, is given by the horizontal lines in Fig. 1. The critical field condition $F = F_c$ corresponds to $\mathcal{E}_I = \mathcal{E}_D$ and is illustrated in Fig. 1(b). In Fig. 1(c) we also indicate the value of the $B = 0$ energies by a thin dotted line, and we note that under a 10 T magnetic field $\mathcal{E}_I$ is raised by 2 meV, while $\mathcal{E}_D$ undergoes a comparatively negligible shift (by 0.13 meV). Fig. 2(a) shows the energy shifts, $\Delta E(B) = \mathcal{E}_I(B) - \mathcal{E}_I(0)$, for three particular values of d: As expected, the effect of the magnetic field is stronger for larger d.

Consequences of this shift in energy are shown in Figs. 2(b) and (c) where we give the expectation value of the z-coordinate of the electronic ground state $\Psi_0 = C_I\Psi_I + C_D\Psi_D$. We start with an electric field slightly above $F_c(d)$, hence, $C_I \approx 1$ and $C_D \approx 0$. Under an increasing magnetic field, the energy shift at the interface eventually detunes $\mathcal{E}_D$ and $\mathcal{E}_I$ in such a way that $C_I \approx 0$ and $C_D \approx 1$, i.e. the electron is taken back to the donor moving parallel to the magnetic field $\mathbf{B}$ and against the electric field $\mathbf{F}$. How big a magnetic field is needed for this process to be completed depends on d and on the value of the static electric field. For those donors further from the interface, the passage of the electronic ground state from the W_I to W_D occurs more abruptly as a function of B. The effect of the value of the electric field is also relevant, as illustrated in Fig. 2(b) and (c). In Fig. 2(b), $F = F_c + 60$ V/cm and the passage occurs around $B \sim 2.2$ T, while in Fig. 2(c), $F = F_c + 120$ V/cm and the needed field is $B \sim 3.2$ T. Therefore, fine tuning of the electric field is required to observe this phenomenon at reasonably small magnetic fields. We propose to use this result as a means of differentiating donor electrons from other charges that may be detected [10] in the architecture shown in Fig. 1(a). Tunneling times are not significantly affected upon magnetic fields considered here and remain a function of d alone [9].

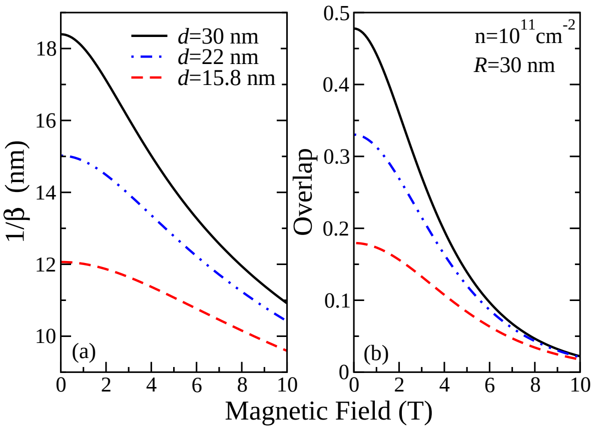

FIG. 3: (Color online) (a) Reduction of the lateral confinement length of the interface state, $1/\beta$, when a perpendicular magnetic field is applied. The effect is stronger for donors that are further away from the interface. (b) Overlap S versus magnetic field for inter-donor separation $R = 30nm$ (which corresponds to a planar density $n = 10^{11}\text{cm}^{-2}$).

The other significant effect of the magnetic field on the interface states is the transverse shrinkage of the wave function. Fig. 3(a) shows the lateral confinement length $1/\beta$ as a function of the magnetic field. For $d = 15.8$ nm, the wave-function width is reduced by a factor of 0.8 when a 10 T magnetic field is applied, while for $d = 30$ nm a stronger reduction factor of 0.6 is obtained. The significance of this enhanced confinement may be accessed through the overlap between interface electrons coming from neighboring donors separated a distance R. The overlap quantifies whether we can consider these electrons as separate entities or they will form a 2-dimensional electron gas (2DEG). One obtains $S = \langle g_\beta(\vec{\rho})|g_\beta(\vec{\rho} + \vec{R})\rangle = \exp(-\beta^2R^2/4)\exp[-R^2/(16\lambda_B^4\beta^2)]$ where we note that, due to gauge invariance, $g_\beta(x+R,y) = \pi^{-1}\beta\exp\{-\beta^2[(x+R)^2+y^2]/2\}\exp\{iyR/(4\lambda_B^2)\}$. The results for the particular inter-donor distance $R = 30$ nm, which corresponds to a planar density $n \sim 10^{11}$ cm^{-2}, are shown in Fig. 3(b). We estimate that an overlap $S \lesssim 0.1$

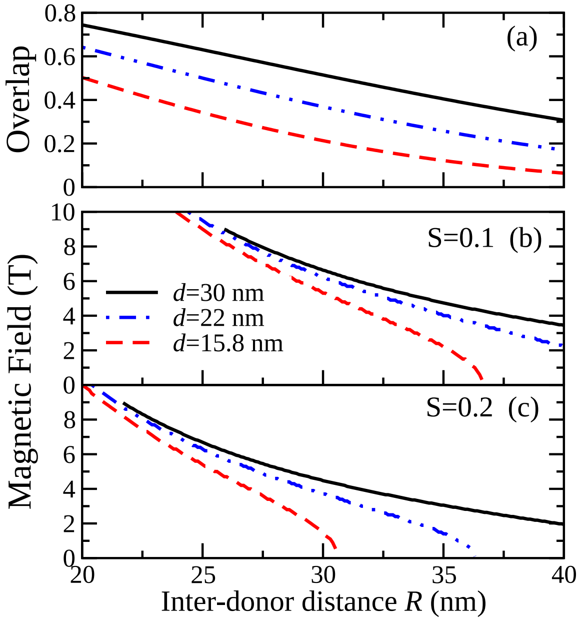

FIG. 4: (Color online) (a) Overlap versus interdonor distance. (b) and (c) show the magnetic field required to reduce the overlap to 0.1 and 0.2 respectively. $R = 20$ nm corresponds to a planar density $n = 2.5 \times 10^{11}$ cm^{-2} and $R = 40$ nm to $n = 6.25 \times 10^{10}$ cm^{-2}.

would guarantee that the electrons do not form a 2DEG. Fig. 4(a) presents the overlap versus inter-donor distance for $B = 0$. The calculated S is generally very large for the experimentally reasonable distances d and R considered here. For the donors further from the interface ($d = 30$ nm), the condition $S < 0.1$ requires either the application of a magnetic field (around 6 T for $R = 30$ nm) or a smaller planar density $n \lesssim 3 \times 10^{10}$ cm^{-2} (which corresponds to $R \gtrsim 55nm$). The magnetic fields required to get a reduction of the overlap to $S = 0.1$ and 0.2 are shown in Fig. 4(b) and (c), respectively, as a function of the inter-donor distance. For the donors closer to the interface ($d = 15.8$ nm), the effect of the magnetic field is not as dramatic: The lateral confinement provided by the donor potential is strong enough to give $S = 0.1$ for $B = 0$ and $R \sim 37$ nm ($n \sim 7.4 \times 10^{10}$ cm^{-2}). Note that in the case of neighboring donors placed at different distances from the interface d, $S(R)$ would present oscillations due to valley interference effects [11].

For qubits defined at the donor sites it is certainly more reliable to perform operations involving two-qubit entanglement at the more directly accessible interface region. In this case, depending on R and d, the confining potential provided by the donors may need to be complemented by additional surface gates [12] and/or static magnetic fields. Time-dependent magnetic fields can be invoked in switching the exchange gates for two-qubit operations [5].

In summary, we demonstrate here that, in addition to the control of donor charges by electric fields, as usual in conventional semiconductor devices, relatively moderate magnetic fields (up to 10 T) may provide relevant information and manipulation capabilities as the building blocks of donor-based QC architectures in Si are being developed. Uniform magnetic fields may displace donor-bound electrons from the interface to the donor nucleus region, as illustrated in Fig. 2. This effect, which could be monitored via surface charge detectors, allows differentiating donor electrons from spurious surface or oxide-region bound electrons, which would not exhibit this type of behavior. For electrons originating from neighboring donors and drawn to the surface by an electric field, the magnetic field lateral confinement effect may provide isolation between electrons (see Fig. 3), allowing smaller interdonor distances to be exploited (see Fig. 4), as well as additional control in two qubits operations via surface exchange gates similar to the spin manipulation in quantum dots in GaAs. Defects such as dangling bonds at the Si/SiO$_2$ interface are important sources of spin decoherence, thus spin coherence times near the interface are expected to be significantly reduced as compared to the bulk. Performing two-qubit (spin-spin) entanglement near the SiO$_2$ interface, as suggested here, requires extremely careful interface optimization. We believe that the use of an external magnetic field along with the FET geometry near a Si-SiO$_2$ interface should allow in the near future significant experimental progress in the currently stalled, but potentially important, donor qubit based Kane spin QC architecture.

This work is supported by LPS and NSA. BK acknowledges support by CNPq and FAPERJ.

[1] R. de Sousa and S. Das Sarma, Phys. Rev. B **68**, 115322 (2003).

[2] W. Witzel, R. de Sousa, and S. Das Sarma, Phys. Rev. B **72**, 161306 (2005).

[3] E. Abe, K. Itoh, J. Isoya, and S.Yamasaki, Phys. Rev. B **70**, 033204 (2004); A. M. Tyryshkin, J. J. L. Morton, S. C. Benjamin, A. Ardavan, G. A. D. Briggs, J. W. Ager, and S. A. Lyon, cond-mat/0512705 (2005).

[4] J. R. Petta, A. C. Johnson, J. M. Taylor, E. A. Laird, A. Yacoby, M. D. Lukin, C. M. Marcus, M. P. Hanson, and A. C. Gossard, Science **309**, 2180 (2005); A. C. Johnson, J. R. Petta, J. M. Taylor, A. Yacoby, M. D. Lukin, C. M. Marcus, M. P. Hanson, and A. C. Gossard, Nature **435**, 925 (2005); T. Hatano, M. Stopa, and S. Tarucha, Science **309**, 268 (2005).

[5] D. Loss and D. P. DiVincenzo, Phys. Rev. A **57**, 120 (1998); G. Burkard, D. Loss, and D. P. DiVincenzo, Phys. Rev. B **59**, 2070 (1999); X. Hu and S. Das Sarma, Phys. Rev. A **61**, 062301 (2000).

[6] B. E. Kane, Nature **393**, 133 (1998).

[7] T. Schenkel, A. Persaud, S. J. Park, J. Nilsson, J. Bokor, J. A. Liddle, R. Keller, D. H. Schneider, D. W. Cheng, and D. E. Humphries, J. Appl. Phys. **94**, 7017 (2003);

S. R. Schofield, N. J. Curson, M. Y. Simmons, F. J. Rueß, T. Hallam, L. Oberbeck, and R. G. Clark, Phys. Rev. Lett. **91**, 136104 (2003); D. Jamieson, C. Yang, T. Hopf, S. Hearne, C. Pakes, S. Prawer, M. Mitic, E. Gauja, S. Andresen, F. Hudson, A. Dzurak, R. Clark, Appl. Phys. Lett. **86**, 202101 (2005).

[8] D. MacMillen and U. Landman, Phys. Rev. B **29**, 4524 (1984); G. Kramer and R. Wallis, Phys. Rev. B **32**, 3772 (1985)

[9] M. Calderón, B. Koiller, X. Hu, and S. Das Sarma, Phys. Rev. Lett. **96**, 096802 (2006).

[10] B. E. Kane, MRS Bulletin **30**, 105 (2005); K. Brown, L. Sun, and B. Kane, cond-mat/0601553 (2006).

[11] B. Koiller, X. Hu, and S. Das Sarma, Phys. Rev. B **66**, 115201 (2002).

[12] For typical values of R and d, the double-well potential from the donor pair alone usually provides a relatively shallow barrier, resulting in negligibly small values of J. Surface gates between the donors could raise the barrier and allow closer donor (smaller R) geometries, leading to values of J compatible with the required gating times ($\hbar/J \ll \sim$ ms), similar to the situation in GaAs quantum dot quantum computing architectures (Ref. 4).